Chapter 17

Prism Resonators

17.1 Porro Prism Resonators

Stable resonators as well as unstable resonators exhibit a relatively high sensitivity to mirror misalignment. Typical tilt angles at which the output power has decreased by 10% are in the range between 0.1mrad and 1mrad. In some applications these angles may be too low to ensure a reliable performance over a long period of time. The misalignment sensitivity can be decreased considerably by using prisms as the resonator mirrors. For a right-angle prism (Porro prism), an incident ray is reflected back parallel to its propagation direction, independent of the angle of incidence (Fig.17.1). A planar wave front remains planar after the reflection by the prism. Except for the mirroring at the prism edge and the change in polarization, a Porro prism exhibits the same imaging properties as a flat, high-reflecting mirror. It is for this reason that high-reflecting resonator mirrors can be replaced by Porro prisms [5.5,5.7,5.8,5.13-5.15]. Mirror curvatures can be simulated by using a curved prism interface. If one prism is used in the resonator set-up, the laser beam is coupled out conventionally through the output coupling mirror (Fig.17.2a). With both resonator mirrors replaced by roof prisms, the output coupling is realized by using a retardation plate in combination with a polarizer (Fig. 17.2b). The rotation of the retardation plate leads to a variation of the output coupling (see also Chapter 8), which means that the output coupling can be adjusted to its optimum value. The decrease in misalignment sensitivity, however, is only attained for a tilt around the roof edge. A tilt of the prism around the perpendicular axis results in the same sensitivity as that of a flat mirror. In order to attain a low misalignment sensitivity with respect to arbitrary tilt axes, a corner cube prism has to be used.

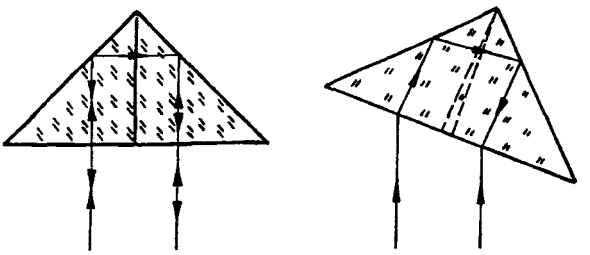

Fig. 17.1 Reflection of a light ray by a Porro prism.

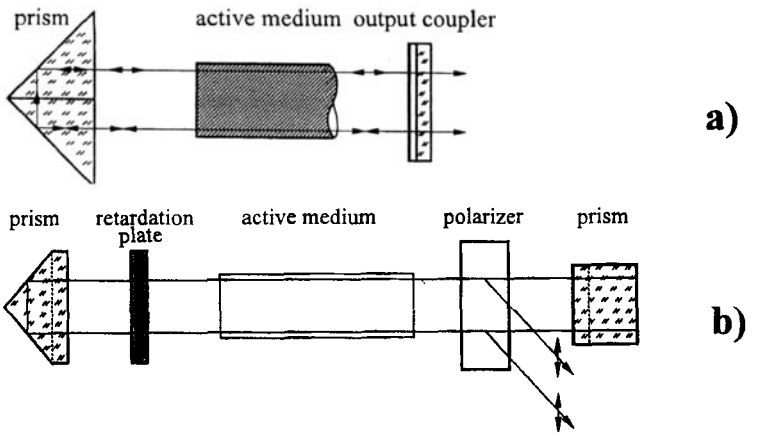

Fig. 17.2 Porro prism resonators with one (a) and two prisms (b). If two prisms are used, the radiation is coupled out of the resonator by means of a polarizer and a rotatable retardation plate.

The beam quality of the laser resonator is not affected by the prism, which means that the same beam parameter product is attained if the prism is replaced by a conventional resonator mirror (Fig. 17.3a). However, depending on the optical quality of the prism, the diffraction losses may be slightly increased due to output coupling and phase distortions induced at the prism edge (Fig. 17.3b). For high quality prisms, which exhibit edge widths of less than 5μm, the additional loss per round trip is less than 0.5%. In this case, the extraction efficiency is as high as for a conventional resonator provided that the small-signal gain is chosen high enough.

The misalignment of the Porro prism around an axis parallel to the prism edge results in a decrease of the mode volume in the active medium (Fig. 17.4). For a resonator in multimode operation, the smaller mode volume is the only cause for the decrease of the output power, since additional diffraction losses are only generated if the fundamental mode gets clipped by the active medium. A simple geometrical analysis yields for the angle $\beta_{10\%}$, at which the mode volume, and consequently the output power, have decreased by 10%:

$$\beta_{10\%} = \frac{0.025\ \pi\ b}{d\ -\ h(1-1/n)} \tag{17.1}$$

with:
- b : radius of the active medium
- d : distance of the tilt axis to the prism edge
- h : prism height
- n : refractive index of prism material

For a radius b of the active medium of 3.15mm and a glass prism ($n=1.5$) with a height of $h=20mm$, the 10%-angle is 37mrad if the prism is rotated around the roof edge ($d=0$).

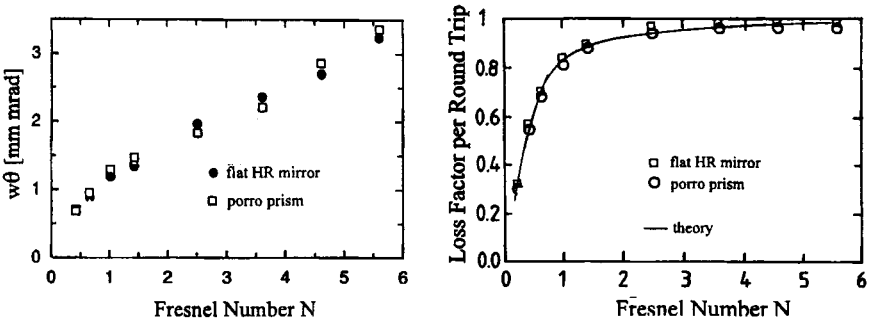

Fig. 17.3 Measured beam parameter product and measured loss factor per round trip for a Nd:YAG rod laser with a flat-flat resonator as a function of the effective Fresnel number N. Measurements with a flat HR mirror and a Porro prism are compared. The output coupling mirror is a conventional flat mirror (see Fig. 17.2a). The effective Fresnel number is given by $N = b^2/(2\lambda L)$ with b: rod radius, L: effective resonator length ($b=3.15mm$, $\lambda=1.064\mu m$). The theoretical loss factor was calculated using diffraction theory.

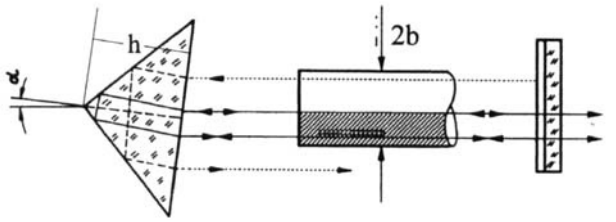

Fig. 17.4 Beam propagation in a misaligned Porro prism resonator. The hatched area indicates the mode volume.

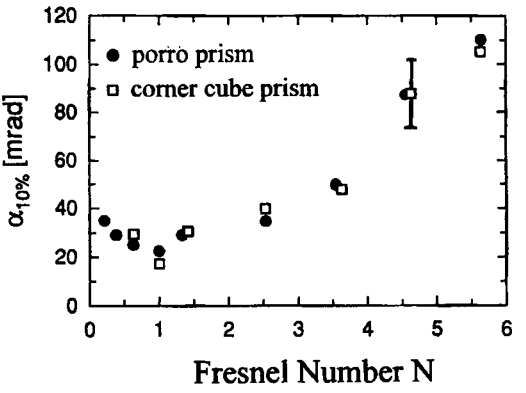

Fig. 17.5 Measured prism tilt angles at which the diffraction losses per round trip have increased by 10% as a function of the effective Fresnel number for a flat-flat resonator with one prism (Porro prism and corner cube prism are compared). The resonator set-up is the one depicted in Fig. 16.2a (Nd:YAG rod laser, rod radius $b=3.15mm$, $\lambda=1.064\mu m$). The effective resonator length is 0.75m, the Fresnel number was varied by using an intracavity aperture. The prisms are rotated around the edge ($d=0$).

The sensitivity to prism misalignment is only low if the prism or the output coupling mirror is rotated around an axis parallel to the roof edge. In order to extend the low sensitivity to both axes, two crossed Porro prisms may be used, as depicted in Fig. 17.6. The output coupling is accomplished by a polarizer in combination with a retardation plate (see also Sec. 8.2.2). The output coupling loss can be calculated by determining the eigenvalues of the Jones matrix for the resonator round trip (see Sec. 1.3). The Jones matrix of a Porro prism is identical to that of a retardation plate since the p-polarized and the s-polarized light exhibit different phase shifts δ_P and δ_S, respectively, due to total internal reflection. According to the Fresnel equations, the net phase shift $\delta=\delta_P-\delta_S$ after two reflections in a Porro prism with index of refraction n is given by:

$$\tan\frac{\delta}{4} = \sqrt{1 - \frac{2}{n^2}} \tag{17.2}$$

Note that the index of refraction must be greater than $\sqrt{2}$ in order to attain total internal reflection at the angle of incidence of 45°. For a BK7 glass prism (n=1.5) the net phase shift amounts to δ=73.7°. Furthermore, an additional phase shift of π has to be taken into account due to the reversal of the beam propagation. The Jones matrix for a Porro prism thus reads:

$$M_{PP}^{P} = \begin{pmatrix} 1 & 0 \\ 0 & \exp[i\Phi] \end{pmatrix} \tag{17.3}$$

with: $\Phi = \delta - \pi$ if the prism edge is parallel to the y-direction
$\Phi = \pi - \delta$ if the prism edge is parallel to the x-direction

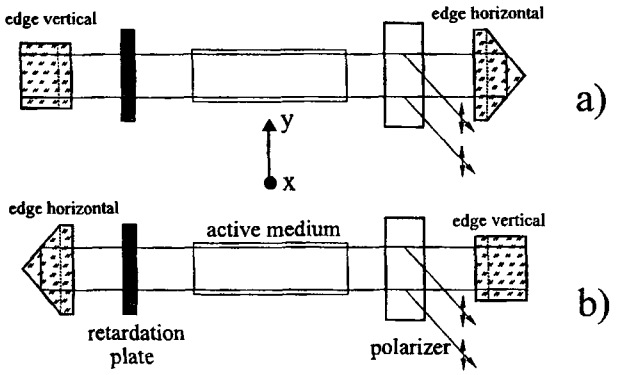

Fig.17.6 Porro prism resonators with crossed prisms. A variable output coupling is achieved by means of a polarizer and a rotatable retardation plate. The p-polarization passes through the polarizer and becomes elliptically polarized after one round trip. The s-polarized portion of the radiation is then reflected by the polarizer.

The resulting Jones matrix yields p-polarized and s-polarized light as the eigenvectors for a round trip. The loss factor V per round trip (1-loss) is given by the square of the eigenvalue for p-polarized light. Provided that the active medium does not affect the polarization, the loss factor reads:

$$V = \left| \left(\cos^2\alpha + \sin^2\alpha \exp[-i\gamma]\right)\exp[i\Phi] + \cos^2\alpha\sin^2\alpha(1-\exp[-i\gamma])^2 \right|^2 \tag{17.4}$$

where α and γ are the angle of rotation and the phase shift of the retardation plate, respectively, and Φ is the phase shift of the left Porro prism (see Fig. 17.6), according to (17.3). Figure 17.7 presents the loss factor per round trip of a Porro prism resonator as a function of the angle of rotation of the retardation plate, calculated with (17.4) using different phase shifts of the retardation plate. The output coupling can be optimized by adjusting the angle of rotation of the retardation plate such that the maximum output power is extracted for a given small-signal gain $g_0\ell$. This adjustment is the second advantage of this resonator scheme, besides the low misalignment sensitivity. Conventional resonators provide optimum output coupling for one fixed value of the small-signal gain only. The loss factor V can be considered as the output coupling reflectance in a conventional resonator. We can therefore use (10.8) in combination with (17.4) to calculate the output power of a Porro prism resonator as a function of the parameters of the retardation plate for a homogeneously broadened active medium:

$$P_{out} = A_b I_S \frac{1-V}{1 - V + \sqrt{V}\,(1/V_S - V_S)} \left[g_0\ell - \left|\ln\sqrt{VV_S^2}\right|\right] \tag{17.5}$$

where A_b is the cross sectional area of the mode in the active medium, I_S is the saturation intensity of the active medium, and V_S is the loss factor per transit due to scattering, absorption, and diffraction. The angles of rotation which provide maximum output power are determined by the equation:

$$\ln V = 2\ln V_S \left[\sqrt{\frac{g_0\ell}{|\ln V_S|} - 1}\right] \tag{17.6}$$

in combination with (17.4). In general, the prism resonator will provide optimum performance at several angles of rotation. An experimental verification of (17.4) is presented in Fig. 17.8 with the corresponding output energy characteristics shown in Fig. 17.9. Note that the difference between a horizontal and a vertical orientation of the left prism is a 90° shift of both the loss factor curve and the output power curve with respect to the angle of rotation of the retardation plate. The right prism does not affect the output coupling at all and may be replaced by a conventional high reflecting mirror.

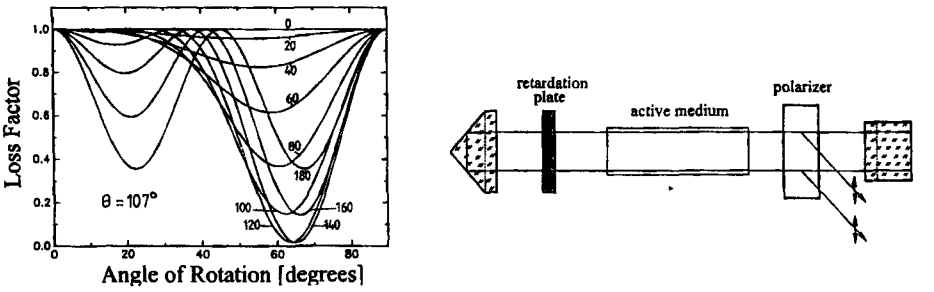

Fig. 17.7 Loss factor per round trip of the depicted Porro prism resonator as a function of the angle of rotation of the retardation plate, calculated with (17.4). The curve parameter is the phase shift γ of the retardation plate. The phase shift of the left Porro prism is Φ=107° (BK7).

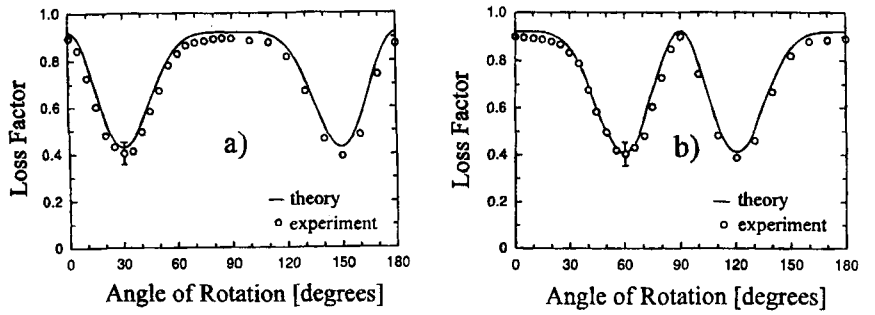

Fig. 17.8 Calculated and measured loss factor per round trip of the prism resonators shown in Fig. 17.6 as a function of the angle of rotation of the retardation plate. The phase shift of the retardation plate is γ=73° and the phase shift of each Porro prism is 73.7°. (Nd:YAG laser with 3"x1/4" rod, single shot operation, effective resonator length L=0.75m, 10% diffraction loss per round trip) [5.21].

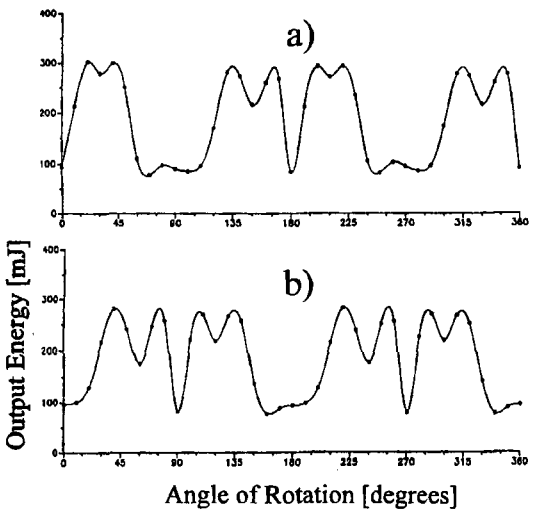

Fig. 17.9 Measured output energy per pulse for the two Porro prism resonators shown in Figs. 17.6 and 17.8 as a function of the angle of rotation of the retardation plate (Nd:YAG laser with 3"x1/4" rod, single shot operation, electrical pump energy : 100J, small-signal gain $g_0\ell$=1.0, effective resonator length L=0.75m) [5.21].

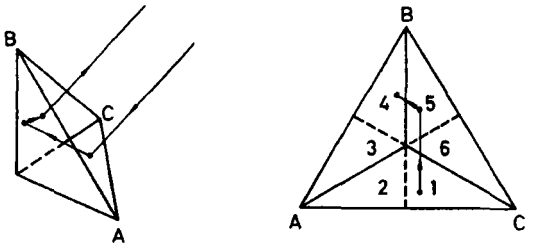

Fig. 17.10 Reflection of a ray by a corner cube prism (side view and front view).

17.2 Corner Cube Prism Resonators

If the high-reflecting mirror is replaced by a corner cube prism, the beam quality and the misalignment sensitivity are the same as for a resonator with one Porro prism (Fig. 17.11 and Fig.17.4). However, the corner cube can be tilted around any axis perpendicular to the optical axis whereas the Porro prism exhibits a low misalignment sensitivity only when rotated around an axis parallel to the prism edge. Furthermore, the corner cube prism resonator exhibits a higher diffraction loss per round trip compared to a Porro prism resonator, as shown in Fig. 17.11. This increase in the loss is a result of the geometry of the corner cube (Fig. 17.10) and is not generated by scattering or output coupling losses at the edges. For a high quality corner cube with typical edge widths on the order of μm, these losses are negligible. Three different modes oscillate independently in a corner cube prism resonator. Each of these modes experience reflections in different areas of the corner cube prism. If we look towards the corner cube prism in direction of the beam propagation, as shown in Fig. 17.10, the three different beams can be related to reflections at the areas 1-5-4, 2-4-5, and 3-1-6, respectively. Each of the three modes, therefore, is controlled by an effective aperture given by one of the six segments of the corner cube. Thus, the effective Fresnel number is lower than the Fresnel number defined by the size of the active medium, resulting in a higher diffraction loss.

The phase shift experienced due to the total internal reflection in the corner cube is different for each of the three modes. This difference in phase shift in combination with the transverse separation is the reason that the three modes establish themselves. The phase shift experienced at each surface can be evaluated by a simple geometrical analysis. Regardless of which surface of the corner cube prism is considered, the angle of incidence of the beam is always 54.4°. Each reflection generates the same phase shift δ between the p-polarization and the s-polarization, given by:

$$\tan\frac{\delta}{2} = \frac{\cos\theta\,\sqrt{\sin^2\theta - 1/n^2}}{\sin^2\theta} \tag{17.7}$$

where θ is the angle of incidence on the surface and n is the index of refraction of the

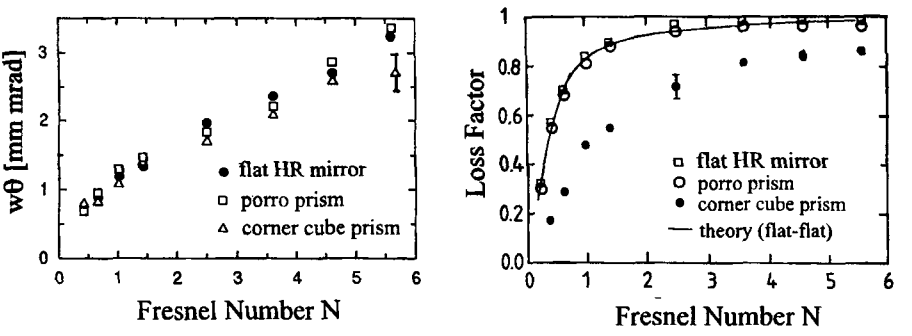

Fig. 17.11 Measured beam parameter product (w: waist radius, θ: half angle of divergence) and measured loss factor per round trip for a Nd:YAG rod laser with a flat flat resonator as a function of the effective Fresnel number N. Measurements with a flat HR mirror, a Porro prism and a corner cube prism are compared. The output coupling mirror is a conventional flat mirror (see Fig. 17.3 for comparison). The effective Fresnel number is given by $N = b^2/(2\lambda L)$ with b: aperture radius, L: effective resonator length (L=0.75m, λ=1.064μm) [5.21].

corner cube prism (δ=44.6° for n=1.5). The phase difference between the three modes is a result of the different orientations of the surface normals with respect to the wave vector incident on each surface. A round trip analysis of the polarization properties of a corner cube prism resonator, therefore, requires the evaluation of a Jones matrix for each of the three possible reflection paths inside the corner cube prism.

Let us consider the reflection at the areas 1-5-4 and determine the Jones matrix for beams incident upon section 1 or 4 of the corner cube prism. The Jones matrices for the other two reflection geometries can be obtained by performing a rotation of the corner cube prism around the optical axis by ±120°. In order to match the orientation of the next reflecting surface, the coordinate system has to be rotated by +60° after the first reflection (at surface 1) and by -60° after the reflection at surface 5. After the final reflection at surface 4, the coordinate system has to be transformed back into the coordinate system of the resonator. The combination of the rotation matrices with the three Jones matrices for the reflections results in the final Jones matrix:

$$\boldsymbol{M}_{1\text{-}4}^{P} = \frac{1}{8}\begin{pmatrix} 1 & -\sqrt{3} \\ -\sqrt{3} & -1 \end{pmatrix}\begin{pmatrix} 1 & 0 \\ 0 & z \end{pmatrix}\begin{pmatrix} 1 & \sqrt{3} \\ -\sqrt{3} & 1 \end{pmatrix}\begin{pmatrix} 1 & 0 \\ 0 & z \end{pmatrix}\begin{pmatrix} 1 & -\sqrt{3} \\ \sqrt{3} & 1 \end{pmatrix}\begin{pmatrix} 1 & 0 \\ 0 & z \end{pmatrix}$$

$$= \frac{1}{8}\begin{pmatrix} 1+6z-3z^2 & -\sqrt{3}(z+2z^2+z^3) \\ -\sqrt{3}(1+2z+z^2) & z(3-6z-z^2) \end{pmatrix} \quad ; \quad z=\exp[i\delta] \tag{17.8}$$

The Jones matrix $\boldsymbol{M}_{4\text{-}1}$ for the reversed beam path is the same. The other two Jones matrices are found by rotating the corner cube by ±120°:

$$M_{2\text{-}5} = M_{5\text{-}2} = \frac{1}{4}\begin{pmatrix} -1 & -\sqrt{3} \\ \sqrt{3} & -1 \end{pmatrix} M_{1\text{-}4} \begin{pmatrix} -1 & \sqrt{3} \\ -\sqrt{3} & -1 \end{pmatrix} \tag{17.9}$$

$$M_{3\text{-}6} = M_{6\text{-}3} = \frac{1}{4}\begin{pmatrix} -1 & \sqrt{3} \\ -\sqrt{3} & -1 \end{pmatrix} M_{1\text{-}4} \begin{pmatrix} -1 & -\sqrt{3} \\ \sqrt{3} & -1 \end{pmatrix} \tag{17.10}$$

In order to determine the output coupling loss of a corner cube prism resonator with variable output coupling using a rotatable retardation plate and a polarizer (see resonator scheme in Fig. 17.12), the eigenvalues of the Jones matrix for a resonator round trip have to be calculated for each of the three modes. For the mode which is incident on segment 1 or segment 4 of the corner cube prism, for instance, the round trip Jones matrix, starting at the polarizer, reads:

$$M_1^P = \begin{pmatrix} 1 & 0 \\ 0 & 0 \end{pmatrix} M_{\lambda/4}^P(\alpha)\, M_{1\text{-}4}^P\, M_{\lambda/4}^P(\alpha) \begin{pmatrix} 1 & 0 \\ 0 & 0 \end{pmatrix} \tag{17.11}$$

where $M_{\lambda/4}^P(\alpha)$ is the Jones matrix of the quarter wave plate as a function of the angle of rotation α (see (3.13)). The two other Jones matrices are obtained by replacing $M_{1\text{-}4}^P(\alpha)$ with the corresponding expressions (17.9) and (17.10).

Figure 17.12 presents the calculated loss factors per round trip for the three modes reflection paths as a function of the angle of rotation of a quarter wave plate (the loss factor represents the output coupling reflectance of the polarizer). The average loss factor shown in the right graph indicates that a rotation of the retardation plate will not have much effect on the output power, provided that all three modes are well above the laser threshold. An experimental verification of this statement is given in Fig. 17.13 for a Nd:YAG rod laser with a small-signal gain of 2. Considering this property, output coupling via polarization does not seem to be advantageous at all. However, since the different modes exhibit different output coupling reflectances, it is possible to control their relative power content by rotating the retardation plate. This may be interesting if a laser system operating at three different wavelengths is considered (i.e. operation of Nd:YAG at 946nm, 1064nm, and 1320nm). By subdividing the flat mirror into six segments using wavelength selective coatings, the emission of the laser can be distributed over the three wavelengths. If the small-signal gain of the medium is not too high, emission at one, two, or three wavelengths can be attained simply by rotating the retardation plate. An experimental example of this mode-switching behavior is presented in Fig. 17.14. The recorded near field intensity distributions of a Nd:YAG laser are shown for different angles of rotation of the retardation plate in this figure.

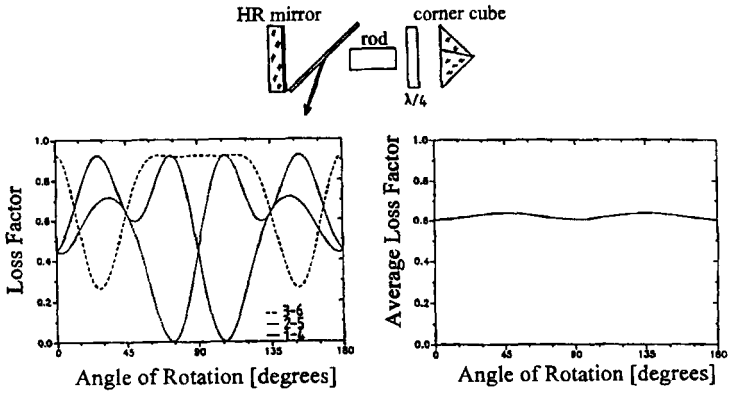

Fig. 17.12 Calculated loss factor per round trip for a corner cube prism resonator with an internal polarizer as a function of the angle of rotation of the quarter wave plate. The loss factor corresponds to the output coupling reflectance of the resonator. The left graph shows the loss factor for the three different modes, the right graph is the mean loss factor, averaged over the three modes.

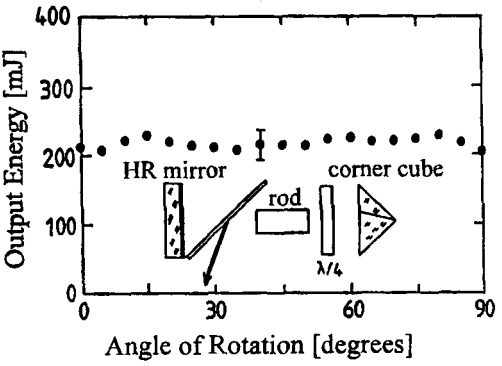

Fig. 17.13 Measured output energy per pulse of a Nd:YAG laser with a corner cube prism resonator as a function of the angle of rotation of the quarter wave plate. (3"1/4" rod, small-signal gain $g_0\ell=1.0$, single shot operation, pulse duration: 500 μs).

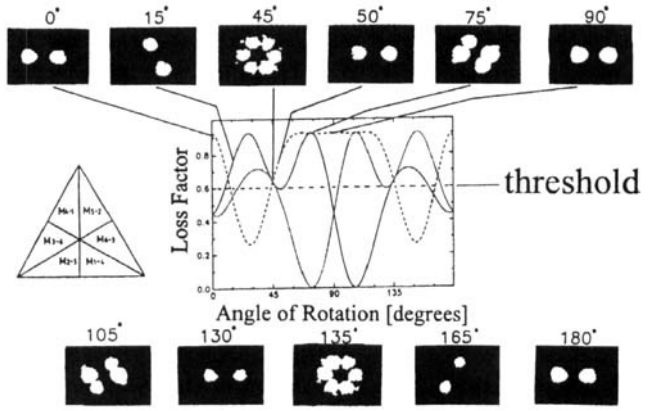

Fig. 17.14 Photographs of the near field intensity of the Nd:YAG laser used in Fig. 17.13 for different angles of rotation of the quarter wave plate. The small-signal gain is $g_0\ell=0.3$, which means that the loss factor must be higher than 0.6 for a mode to exceed the laser threshold (5% loss per transit) [S.10].